Synthesis and diphosphine ligand fluxionality in $Os_3(CO)_{10}(bmi)$: Kinetic evidence for nondissociative diphosphine isomerization and X-ray crystal structure of $1,1-Os_3(CO)_{10}(bmi)$

William H. Watson [a],*, Bhaskar Poola [b], Michael G. Richmond [b],*

[a] *Department of Chemistry, Texas Christian University, Fort Worth, TX 76129, United States*
[b] *Department of Chemistry, University of North Texas, P.O. Box 305070, Denton, TX 76203-5070, United States*

Abstract

The triosmium cluster $1,2-Os_3(CO)_{10}(MeCN)_2$ reacts rapidly with the diphosphine ligand *2,3*-bis(diphenylphosphino)-N-*p*-tolylmaleimide (bmi) at room temperature to give bmi-bridged cluster $1,2-Os_3(CO)_{10}(bmi)$ (**2b**) as the major product, along with the chelating isomer $1,1-Os_3(CO)_{10}(bmi)$ (**2c**) and the hydride-bridged cluster $HOs_3(CO)_9[\mu-(PPh_2)C=C\{PPh(C_6H_4)\}C(O)N(tolyl-p)C(O)]$ (**3**) as minor by-products. All three cluster compounds have been isolated and fully characterized in solution by IR and NMR spectroscopies (^{1}H and ^{31}P), and X-ray crystallography in the case of **2c**. Cluster **2b** is unstable and readily isomerizes to **2c** in quantitative yield on mild heating. The kinetics for the conversion of $\mathbf{2b} \rightarrow \mathbf{2c}$ have been measured over the temperature range of 318–348 K in toluene solution, and based on the observed activation parameters a nondissociative isomerization process that proceeds via a transient μ_2-bridged phosphine moiety is presented. Near-UV photolysis of cluster **2c** at room temperature affords $HOs_3(CO)_9[\mu-(PPh_2)C=C\{PPh(C_6H_4)\}C(O)N(tolyl-p)C(O)]$ (**3**) with a quantum yield of 0.017. The reactivity of clusters **2b**, **2c**, and **3** is discussed with respect to related diphosphine-substituted $Os_3(CO)_{10}(P–P)$ clusters prepared by our groups.
© 2006 Elsevier B.V. All rights reserved.

Keywords: Osmium clusters; Diphosphine ligand fluxionality; Kinetics; Ortho metalation

1. Introduction

The number of reports involving phosphine ligands that are coordinated to organometallic compounds via nonclassical bonding modes has risen sharply over the last several years. Simple phosphine ligands have generally been assumed to function only as terminal ligands that bind to metals through the η^1 coordination mode [1]. Recent structural and mechanistic work from the Balch [2], Werner [3], and Réau [4] groups have unequivocally demonstrated the existence of a wide variety of organometallic compounds possessing μ_2- and μ_3-bridged tertiary phosphine ligands as stable and isolable entities. These elegant examples that involve the ligation of simple phosphine ligands to multiple metal centers are reminiscent of the CO ligand, whose rich coordination chemistry has been thoroughly reviewed [5].

The documentation of stable μ_2- and μ_3-bridged phosphine organometallic compounds suggests that many of the known phosphine-substituted polynuclear compounds may actual exhibit heretofore unrecognized stereodynamic behavior in terms of phosphine ligand fluxionality [6]. Here the permutation of a phosphine ligand(s) between adjacent metal centers may be achieved through analogous μ_2- and μ_3-phosphine intermediates without having to invoke a

* Corresponding authors. Tel.: +1 817 257 7195 (W.H. Watson); tel.: +1 940 565 3548; fax: +1 940 565 4318 (M.G. Richmond).
E-mail addresses: w.watson@tcu.edu (W.H. Watson), cobalt@unt.edu (M.G. Richmond).

dissociative phosphine-off, phosphine-on sequence. Definitive proof has been presented by several research groups for the nondissociative isomerization of mono- and bidentate phosphine ligands at di- and polynuclear metal compounds. Scheme 1 summarizes a few of the well-known systems that exhibit nondissociative phosphine ligand fluxionality [7–10].

Previous research from our groups has dealt with the synthesis and reactivity studies of metal clusters possessing the rigid diphosphine ligands 2,3-bis(diphenylphosphino)maleic anhydride (bma) and 4,5-bis(diphenylphosphino)-4-cyclopenten-1,3-dione (bpcd) [11]. Wishing to probe the effect that the ancillary diphosphine ligand has on the reaction chemistry, viz-á-vis bma and bpcd, we have prepared the related maleimide ligand 2,3-bis(diphenylphosphino)-N-p-tolylmaleimide (bmi) and have investigated the substitution chemistry of this new ligand with the triosmium cluster 1,2-$Os_3(CO)_{10}(MeCN)_2$. We have previously examined the substitution chemistry of the related diphosphine ligand 2,3-bis(diphenylphosphino)-N-phenyl-maleimide (bppm)

with $Ru_3(CO)_{12}$, as outlined in Eq. (1) [12]; however, the five phenyl groups belonging to the bppm ligand seriously hampered a detailed kinetics investigation due to overlapping aromatic proton resonances. Accordingly, we have synthesized the closely related maleimide-based ligand bmi that bears a N-tolyl group. The p-methyl moiety associated with the N-tolyl group serves as a suitable probe handle that will allow us to follow the progress of our reactions by ^1H NMR spectroscopy. Herein we report our results on the reaction between cluster **1** and bmi, which gives 1,2-$Os_3(CO)_{10}$(bmi) (**2b**) as the principal product, in addition to 1,1-$Os_3(CO)_{10}$(bmi) (**2c**) and the hydride-bridged cluster $HOs_3(CO)_9[\mu-(PPh_2)C=C\{PPh(C_6H_4)\}C(O)N(tolyl-p)C(O)]$ (**3**). These new clusters have been fully characterized in solution by spectroscopic methods and X-ray crystallography in the case of **2c**. The kinetics for the isomerization of **2b** → **2c** have been investigated, and the facile ortho metalation of one of the ancillary phenyl groups in **2c** upon near-UV photolysis to give **3** is discussed.
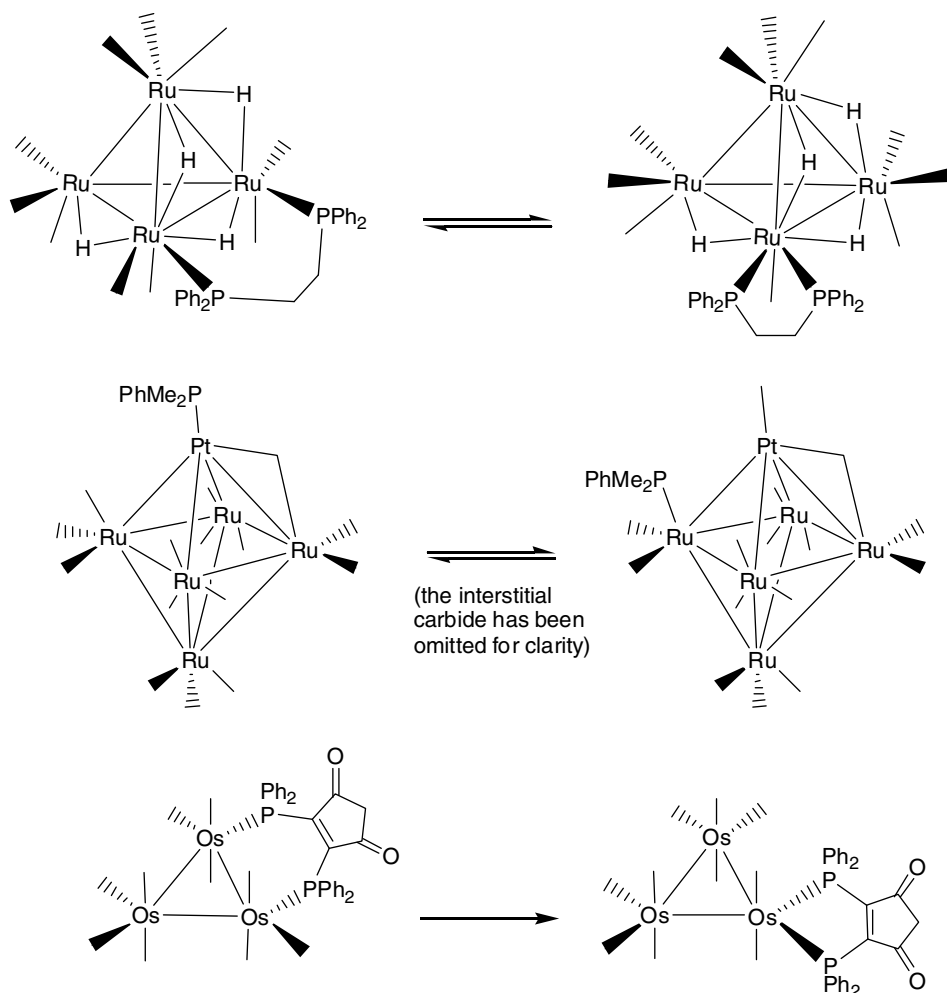
Scheme 1.

(1)
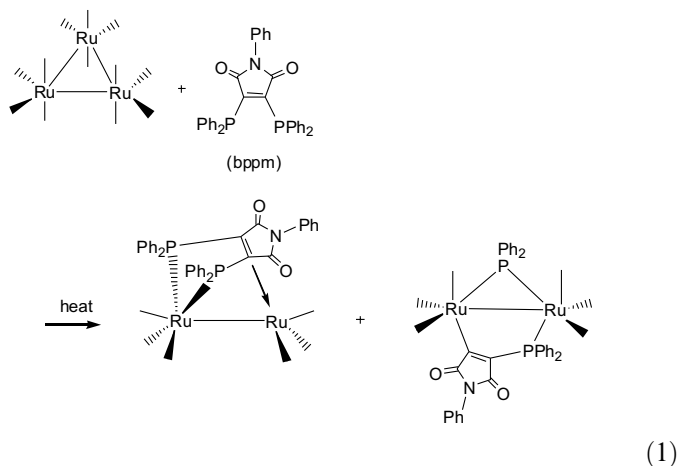
2. Experimental

2.1. General

The acetonitrile-substituted cluster 1,2-$Os_3(CO)_{10}$-(MeCN)$_2$ (1) was prepared from $Os_3(CO)_{12}$ [13], which in turn was obtained from the high-pressure carbonylation of OsO_4 using a 500 mL Parr 4571 series autoclave [14]. The 2,3-dichloro-N-p-tolylmaleimide that was used in the preparation of the bmi ligand was prepared from 2,3-dichloromaleic anhydride and p-toluidine [15]. The chemicals $Me_3NO \cdot xH_2O$, 2,3-dichloromaleic anhydride, and p-toluidine were purchased from Aldrich Chemical Co. The $Me_3NO \cdot xH_2O$ was dried by azeotropic distillation from benzene and the remaining chemicals were used as received. All reaction and NMR solvents were distilled from an appropriate drying agent using Schlenk techniques and stored under argon in storage vessels equipped with a high-vacuum Teflon stopcock [16]. The photolysis experiments were carried out with GE blacklight bulbs having a maximum output of 366 ± 20 nm, and the measured quantum yield for the conversion of 2c → 3 was determined by ferrioxalate actinometry [17]. The combustion analyses were performed by Atlantic Microlab, Norcross, GA.

The IR spectral data were recorded on a Nicolet 20 SXB FT-IR spectrometer in sealed 0.1 mm NaCl cells, while the ^1H and ^{31}P NMR data were recorded at 200 MHz on a Varian Gemini-200 spectrometer and 121 MHz on a Varian 300-VXR spectrometers, respectively. The ^{31}P NMR data were recorded in the proton-decoupled mode, unless otherwise stated, and are referenced to external H_3PO_4, whose chemical shift was set at δ 0.

2.2. Synthesis of 2,3-bis(diphenylphosphino)-N-p-tolylmaleimide (bmi)

To a 250 mL round bottom Schlenk flask was added 0.50 g (2.0 mmol) of 2,3-dichloro-N-p-tolylmaleimide, followed by 7 mL of THF and 60 mL of Et_2O. The solution was next cooled to 0 °C and treated dropwise with 1.10 mL (4.20 mmol) of Ph_2PTMS and stirred at this

temperature for 3 h. At this point the solution was cooled to −78 °C to induce the precipitation of the bmi ligand. The solvents and accompanying TMSCl were then cannulated away from the orange colored ligand, followed by washing with a small amount of hexane to afford pure bmi. Typical yields of bmi are on the order of 90–95%. IR (CH_2Cl_2): $v(CO)$ 1772 (vw, sym maleimide), 1709 (s, antisym maleimide) cm^{-1}. ^1H NMR (CDCl$_3$): δ 2.40 (s, Me), 7.23–7.61 (m, 24H, aromatics). ^{31}P NMR (CDCl$_3$): δ −24.04 (s).

2.3. Synthesis of 1,2-$Os_3(CO)_{10}(bmi)$ from 1,2-$Os_3(CO)_{10}(MeCN)_2$

To 0.25 g (0.27 mmol) of 1,2-$Os_3(CO)_{10}(MeCN)_2$ in 30 mL of CH_2Cl_2 under argon flush was added 0.15 g (0.27 mmol) of bmi in one portion. The reaction was stirred at room temperature for ca. 3 h, at which time TLC analysis confirmed the complete consumption of cluster 1 and the formation of a single green spot at $R_f = 0.60$ (1:1 CH_2Cl_2/hexane) corresponding primarily to 1,2-$Os_3(CO)_{10}(bmi)$ (2b, 80%) and minor amounts of 1,1-$Os_3(CO)_{10}(bmi)$ (1c, 10%) and the hydride-bridged cluster $HOs_3(CO)_9[\mu-(PPh_2)C=C\{PPh(C_6H_4)\}C(O)N(tolyl-p)C(O)]$ (3, 10%). The bmi-substituted clusters 2b, 2c and 3 were obtained by flash column chromatography over silica gel using a 3:7 mixture of CH_2Cl_2/hexane as the eluent. Spectroscopic data for 2b: IR (CH_2Cl_2): $v(CO)$ 2092 (s), 2046 (m), 2011 (s), 1976 (m), 1961 (m), 1778 (vw, sym maleimide), 1720 (s, antisym maleimide) cm^{-1}. ^1H NMR (CDCl$_3$): δ 2.25 (s, Me), 6.90–7.95 (m, 24H, aromatics). ^{31}P NMR (CDCl$_3$): δ −15.36 (s).

2.4. Isomerization of 2b to 2c

The preparative conversion of 2b to 2c may be quantitatively achieved by heating the above mixture containing 2b, 2c, and 3 from 50–60 °C in toluene under 1 atm of CO, whose presence is required to suppresses the formation of the hydride cluster 3 (vide infra). The extent of the isomerization is best followed by NMR spectroscopy. Typical yields of recrystallized 2c were on the order of 80–90%. Spectroscopic data for 2c: IR (CH_2Cl_2): $v(CO)$ 2097 (s), 2045 (s), 2012 (s), 1991 (m), 1978 (m), 1961 (m), 1771 (vw, sym maleimide), 1718 (s, antisym maleimide) cm^{-1}. ^1H NMR (CDCl$_3$): δ 2.36 (s, Me), 7.00–8.30 (m, 24H, aromatics). ^{31}P NMR (CDCl$_3$): δ 24.29 (s). Anal. Calc. for $C_{45}H_{27}NOs_3O_{12}P_2$: C, 38.44; H, 1.94. Found: C, 38.56; H, 2.12%.

2.5. Photochemical preparation of $HOs_3(CO)_9$-$[\mu-(PPh_2)C=C\{PPh(C_6H_4)\}C(O)N(tolyl-p)C(O)]$

To a small Schlenk storage vessel was added 50 mg (0.036 mmol) of cluster 2c and 25 mL of toluene, after which the vessel was sealed and subjected to three freeze–pump–thaw degas cycles. The vessel was next placed

between two GE Blacklights and irradiated until all of the starting cluster had been consumed. Depending on the thickness of the glass tubing used in the construction of the storage vessel, the reaction could be driven to completion over the course of several days. The CO that accompanies the formation of $HOs_3(CO)_9[\mu$-$(PPh_2)C=C\{PPh(C_6H_4)\}C(O)N(tolyl$-$p)C(O)]$ (**3**) was periodically removed by additional freeze–pump–thaw degas cycles. The crude reaction solution containing cluster **3** was passed over a short pad of silica gel and recrystallized from CH_2Cl_2/hexane to furnish **3** as a yellow-green colored solid in 92% yield (44 mg). IR (CH_2Cl_2): ν(CO) 2107 (vs), 2084 (s), 2068 (vs) 2042 (s), 2020 (s), 1985 (s), 1967 (m), 1923 (vs), 1773 (vw, sym maleimide), 1718 (s, antisym maleimide) cm^{-1}. ^{1}H NMR (C_6D_6): δ −15.79 (t, hydride, $J_{P-H} = 14$ Hz), 1.98 (s, Me), 6.50–8.80 (m, 23H, aromatics). ^{31}P NMR (C_6D_6): δ 24.55 (d, $J_{P-P} = 14$ Hz), 33.76 (d, $J_{P-P} = 14$ Hz). Anal. Calc. for $C_{44}H_{27}NOs_3O_{11}P_2$: C, 38.34; H, 1.97. Found: C, 38.40; H, 2.19%.

2.6. X-ray diffraction structure for 1,1-Os₃(CO)₁₀(bmi) (2c)

Single crystals of $1,1$-$Os_3(CO)_{10}$(bmi) were grown from a CH_2Cl_2 of the cluster that had been layered with hexane. The reported X-ray data were collected on a Bruker SMART™ 1000 CCD-based diffractometer at 213 K. The frames were integrated with the available SAINT software package using a narrow-frame algorithm [18], and the structure was solved and refined using the SHELXTL program package [19]. The molecular structure was checked by using PLATON [20], and solved by direct methods with all

Table 1
X-ray crystallographic data and processing parameters for 1,1-Os₃(CO)₁₀(bmi) (2c)

CCDC No.	606514
Space group	Monoclinic, $P2_1/c$
a (Å)	19.488(4)
b (Å)	11.446(2)
c (Å)	19.801(4)
β (°)	102.853(3)
V (Å^3)	4306(1)
Molecular formula	$C_{45}H_{27}NO_{12}Os_3P_2$
Formula weight	1406.22
Formula units per cell (Z)	4
D_{calc} (Mg/m^3)	2.169
λ (Mo Kα) (Å)	0.71073
μ (mm^{-1})	8.969
Crystal size (mm)	$0.29 \times 0.10 \times 0.029$
R_{merge}	0.1144
Absorption correction	Empirical
Absorption correction factor	0.738/0.466
Total reflections	17378
Independent reflections	6188
Data/residual/parameters	6188/0/570
R	0.0748
R_w	0.1807
Goodness-of-fit on F^2	1.113
Largest difference peak and hole (e/Å^3)	3.330 and −2.211

Table 2
Selected bond distances (Å) and angles (°) for 1,1-Os₃(CO)₁₀(bmi) (2c)[a]

Bond distances (Å)

Os(1)–Os(2)	2.922(1)	Os(1)–Os(3)	2.924(1)
Os(2)–Os(3)	2.887(1)	Os(1)–P(1)	2.302(6)
Os(1)–P(2)	2.298(6)	P(1)···P(2)	3.176(8)
Os(1)–C(36)	1.97(3)	Os(1)–C(37)	1.95(3)
Os(2)–C(38)	1.98(3)	Os(2)–C(39)	1.89(3)
Os(2)–(40)	1.84(3)	Os(2)–C(41)	1.87(3)
Os(3)–C(42)	1.89(3)	Os(3)–C(43)	1.93(2)
Os(3)–C(44)	1.90(2)	Os(3)–C(45)	1.88(3)
N(1)–C(1)	1.41(3)	N(1)–C(4)	1.37(3)
N(1)–C(5)	1.43(3)	C(1)–C(2)	1.56(3)
C(2)–C(3)	1.35(3)	C(3)–C(4)	1.56(3)

Bond angles (°)

P(2)–Os(1)–P(1)	87.3(2)	P(2)–Os(1)–Os(2)	168.1(1)
P(1)–Os(1)–Os(2)	104.6(1)	P(2)–Os(1)–Os(3)	109.3(2)
P(1)–Os(1)–Os(3)	160.9(1)	C(2)–P(1)–Os(1)	106.3(7)
C(3)–P(2)–Os(1)	105.9(8)	C(4)–N(1)–C(1)	114(1)
C(4)–N(1)–C(5)	121(2)	C(1)–N(1)–C(5)	125(2)
C(3)–C(2)–P(1)	119(2)	C(2)–C(3)–P(2)	121(2)

[a] Numbers in parentheses are estimated standard deviations in the least significant digit.

nonhydrogen atoms refined anisotropically. All carbon-bound hydrogen atoms were assigned calculated positions and allowed to ride on the attached heavy atom, unless otherwise noted. There was some unresolvable disorder around the osmium atoms that is responsible for the large observed residual peaks. Refinement converged at $R = 0.0748$ and $R_w = 0.1807$ for 6188 independent reflections with $[I > 2\sigma(I)]$. Tables 1 and 2 report the X-ray data collection and processing parameters and selected bond distances and angles for cluster **2c**, respectively.

2.7. Kinetic studies

The UV–vis studies were carried out in toluene solution at a cluster concentration of ca. 10^{-4} M using 1.0 cm quartz UV–vis cells that were equipped with a high-vacuum Teflon stopcock to facilitate handling on the vacuum line. Freshly prepared solutions of **2b** (including minor amounts of **2c** and **3**, vide supra) in toluene were saturated with CO prior to heating to suppress the formation of the hydride-bridged cluster $HOs_3(CO)_9[\mu$-$(PPh_2)C=C\{PPh(C_6H_4)\}C(O)N(tolyl$-$p)C(O)]$. The Hewlett–Packard 8452A diode array spectrometer employed in our studies was configured with a variable-temperature cell holder and was connected to a VWR constant temperature circulator, which regulated the reaction temperature to within ±0.5 K. The ^{1}H NMR kinetics study was conducted in a 5 mm NMR tube that possessed a J-Young valve for the easy admission of CO gas. The NMR study was carried out in toluene-d_8 as a solvent with a cluster concentration of ca. 10^{-2} M. p-Dimethoxybenzene was employed as an internal standard and the exact composition of **2b**, **2c**, and **3** quantified immediately before the start of the reaction. Since the concentration of cluster **3** remained essentially

unchanged over the course of the reaction (<2% conversion to **2c**), the progress of the reaction was monitored by measuring of the area under the tolyl methyl resonance for cluster **2b** at δ 1.83 for slightly over three half-lifes. The NMR sample was heated in the same VWR temperature bath and quenched in an external ice bath immediately before NMR analysis.

The UV–vis kinetics were monitored by following the increase of the 362 nm absorbance band as a function of time for 4–6 half-lifes. The rate constants for the isomerization were determined by non-linear regression analysis using the single exponential function [21]:

$$A(t) = A_\infty + \Delta A^* \exp(-kt)$$

The quoted activation parameters were calculated from plots of $\ln(k/T)$ versus T^{-1} [22], with the error limits representing deviation of the data points about the least-squares line of the Eyring plot.

3. Results and discussion

3.1. Synthesis and spectroscopic data for the bmi-substituted clusters $Os_3(CO)_{10}(bmi)$ and X-diffraction structure of 1,1-$Os_3(CO)_{10}(bmi)$

Treatment of 1,2-$Os_3(CO)_{10}(MeCN)_2$ (**1**) with an equimolar amount of bmi at room temperature leads to the rapid and complete consumption of cluster **1** and furnishes the bmi-bridged cluster 1,2-$Os_3(CO)_{10}(bmi)$ (**2b**) in 80% yield, as determined by ^1H and ^{31}P NMR spectroscopies. Accompanying the formation of **2b** are the clusters 1,1-$Os_3(CO)_{10}(bmi)$ (**1c**) and the $HOs_3(CO)_9[\mu$-$(PPh_2)C=C\{PPh(C_6H_4)\}C(O)N(tolyl-p)C(O)]$ (**3**), each of

which is present in ca. 10% yield. TLC examination of the reaction mixture revealed only one spot for the three cluster products, necessitating the use of NMR spectroscopy to unequivocally establish the composition of the mixture. The major ^{31}P NMR resonance observed at δ −15.36 is in agreement the proposed bmi-bridged cluster **2b** [23], with the dominant methyl singlet appearing at δ 2.25 in the ^1H NMR spectrum (in CDCl₃) readily assigned to cluster **2b**. Since repeated attempts to purify cluster **2b** by recrystallization were not successful, as assessed spectroscopically, we employed the mixture containing **2b**, **2c**, and **3** directly in our reactivity studies. Scheme 2 depicts this reaction and the observed products.

The relationship of these products was next examined by carrying out a few control experiments. Stirring solutions of **1** with bmi for shorter reaction times and/or dropping the reaction temperature down to 0 °C led to a decrease in the yield of **2b** without any significant diminution in relative amounts of clusters **2c** and **3** to **2b**. These results suggest that clusters **2b**, **2c**, and **3** originate from independent pathways. The possibility of the hydride-bridged cluster **3** arising from a room-light promoted ortho metalation involving either **2b** or **2c** (vide infra) was eliminated from contention by performing our experiments in foil-wrapped vessels in the dark and/or under red-light conditions. Here the amount of cluster **3** formed in the two control experiments was not statistically different from the standard reaction between **1** and bmi. Also the thermal conversion of **2b** → **2c** at room temperature may be eliminated from consideration based on the extrapolated rate data from our isomerization studies on **2b** → **2c**, which place the half-life for this conversion at 298 K at over 4 days (vide infra). Accordingly, the **2c** that is observed in our synthetic
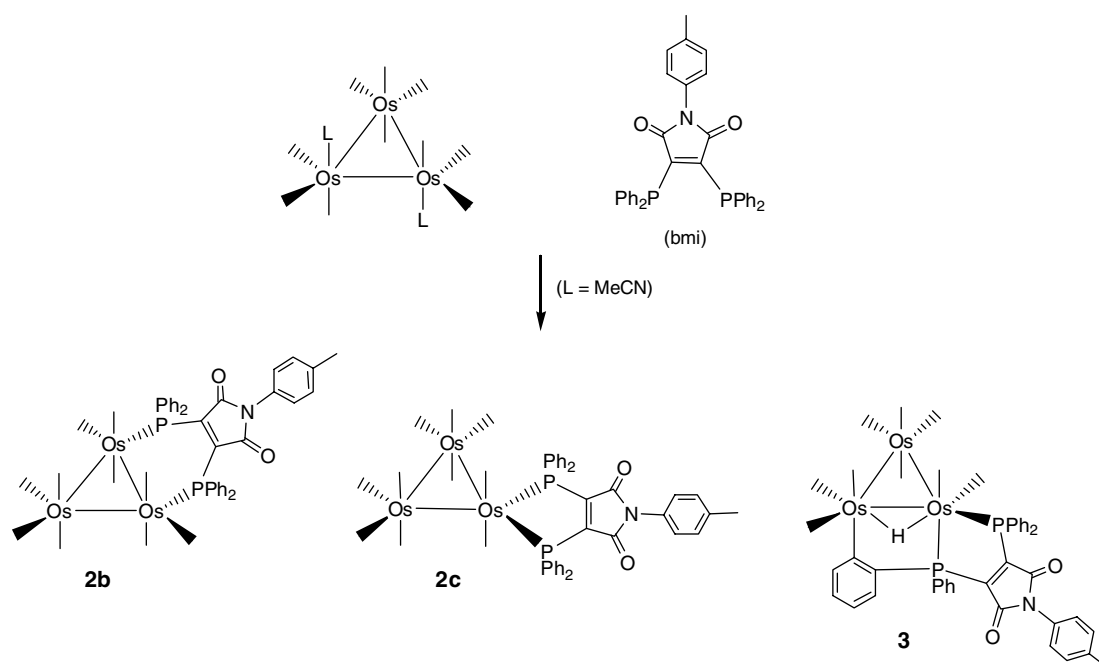
Scheme 2.

reactions must arise from the direct substitution of **1** with bmi. The behavior exhibited by **1** in its reaction with bmi is similar to the bimodal substitution attendant in the reaction of cluster **1** with the diphosphine ligand dmpe, which affords the two clusters 1,2-Os$_3$(CO)$_{10}$(dmpe) and 1,1-Os$_3$(CO)$_{10}$(dmpe) as a non-interconverting isomeric mixture [24].

Heating the initial cluster mixture containing **2b**, **2c**, and **3** in toluene at 60 °C in a thermostated bath for 24 h led to the complete consumption of **2b** and the formation of an 83:17 mixture of clusters **2c** and **3** as determined by ^{1}H NMR spectroscopy [25]. Repeating the thermolysis reaction under 1 atm of CO furnished **2c** in near quantitative yield, paralleling our earlier work on the osmium clusters Os$_3$(CO)$_{10}$(bpcd) and Os$_3$(CO)$_{10}$[(Z)-Ph$_2$PCH=CHPPh$_2$], where added CO suppressed the ortho metalation reaction that affords the hydride clusters HOs$_3$(CO)$_9$[μ-Ph$_2$PC=C{PPh(C$_6$H$_4$)}C(O)CH$_2$C(O)] and HOs$_3$(CO)$_9$[μ-(Z)-Ph$_2$PCH=CH{PPh(C$_6$H$_4$)}] [9,10i]. The IR spectrum of recrystallized **2c** exhibited terminal carbonyl stretching bands at 2097 (s), 2045 (s), 2012 (s), 1991 (m), 1978 (m), 1961 (m) cm^{-1}, along with two lower frequency carbonyl bands at 1771 (vw) and 1718 (s) cm^{-1} belonging to the vibrationally coupled maleimide CO groups [26]. The ^{1}H NMR spectrum in CDCl$_3$ revealed a methyl resonance and aromatic hydrogens at δ 2.36 and 7.00–8.30, respectively, while the down-field singlet recorded at δ 24.29 in the ^{31}P NMR spectrum are collectively in accord with the proposed structure for **2c**.

The unequivocal identity of **2c** was established by X-ray crystallography. The thermal ellipsoid plot of 1,1-Os$_3$(CO)$_{10}$(bmi) is shown in Fig. 1, where the chelation of the bmi ligand to the triosmium frame is confirmed. The three osmium atoms in **2c** form an isosceles triangle with the two longer Os–Os bonds exhibiting distances of 2.922(1) Å [Os(1)–Os(2)] and 2.924(1) Å [Os(1)–Os(3)] and the shorter Os(2)–Os(3) bond displaying a distance of 2.887(1) Å. The mean osmium-osmium bond distance of 2.911 Å is in agreement with those metal–metal bond distances in related polynuclear osmium clusters [27]. The two longer Os–Os bonds are each *cis* to one of the phosphorus atoms on the bmi-chelated osmium atom in agreement with the general trend regarding P-ligand induced elongation of *cis* metal–metal bonds in triangular metal clusters [27d,28]. The two Os–P bond lengths of 2.298(6) Å [Os(1)–P(1)] and 2.302(6) Å [Os(1)–P(2)] are not statistically different and fall within an acceptable range for Os–P bond distances. The P(1)–Os(1)–P(2) bond angle of 87.3(2)° and the internuclear P(1)···P(2) distance of 3.176(8) Å are not unusual in comparison to those values found by us for other chelated diphosphine ligands of this genre [29]. The 10 ancillary CO groups are all linear and exhibit normal distances, and the twist angle formed by the tolyl ring carbons and the maleimide ring is 57.9(9)°, confirming that the two rings are not coplanar. The remaining bond distances and angles are unexceptional and require no comment.
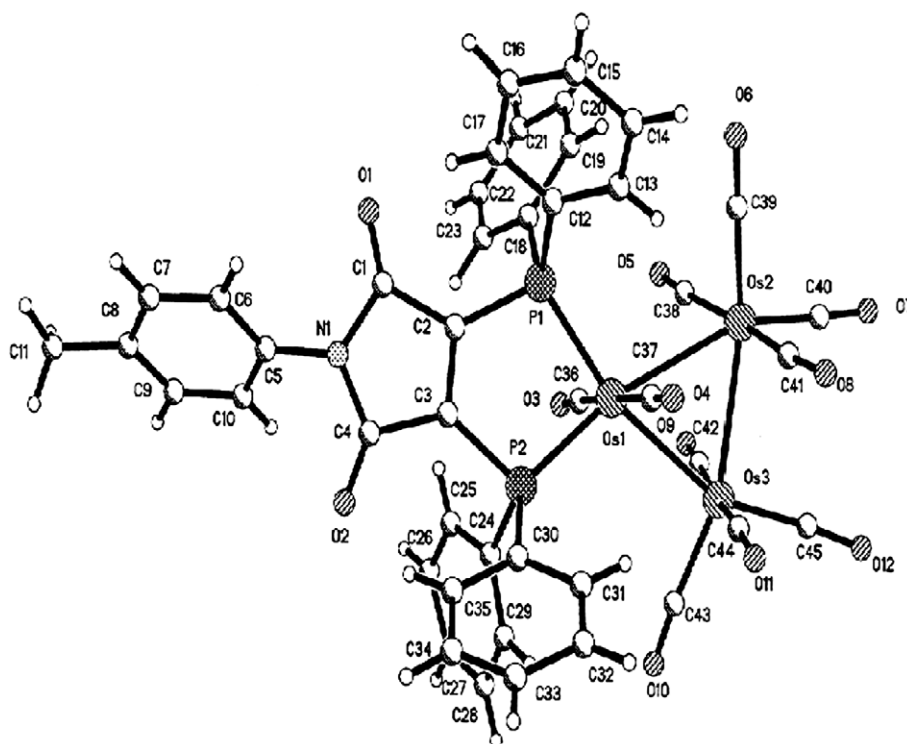

Fig. 1. Thermal ellipsoid plot of 1,1-Os$_3$(CO)$_{10}$(bmi) (**2c**) showing the thermal ellipsoids at the 50% probability level.

3.2. Photochemical activation of 1,1-Os$_3$(CO)$_{10}$(bmi) and formation of the hydride cluster HOs$_3$(CO)$_9$-[μ-(PPh$_2$)C=C{PPh(C$_6$H$_4$)}C(O)N(tolyl-p)C(O)]

The formation of HOs$_3$(CO)$_9$[μ-(PPh$_2$)C=C{PPh-(C$_6$H$_4$)}C(O)N(tolyl-p)C(O)] from 1,1-Os$_3$(CO)$_{10}$(bmi) was next established by near-UV photolysis of the latter chelating cluster. Irradiation of **2c** in toluene solution with 366 nm light leads to CO loss and formation of **3**, as assessed by NMR and UV–vis spectroscopies. Fig. 2 shows the UV–vis changes from a typical photolysis experiment conducted at room temperature. Here the decrease in the absorbances at 362 and 437 nm belonging to **2c** are accompanied by an increase in the 392 nm band for the hydride cluster **3**. The clean conversion of **2c → 3** is further strengthened by the isosbestic points at 387 and 421 nm in the UV–vis spectral traces. The measured quantum yield of 0.017 for the formation of **3** is identical to the value reported by us for the ortho metalation of 1,1-Os$_3$(CO)$_{10}$(bpcd) ($\Phi = 0.02$) [9]. Cluster **3** was obtained in high yield from a preparative photolysis of **2c** and fully characterized in solution by IR and NMR spectroscopies and combustion analysis. The ^{1}H NMR spectrum of **3** in C$_6$D$_6$ exhibits three sets of resonances at δ −15.79, 1.98, and 6.50–8.80 ascribed to the bridging hydride, Me group, and aromatic hydrogens, respectively, while the ^{31}P NMR spectrum displays a pair of inequivalent ^{31}P resonances at δ 24.55 and 33.76. These spectroscopic data are fully consistent with the proposed structure for **3** [30]. Finally, thermolysis of **3** at 60–65 °C under 1 atm of CO regenerates cluster **2c**, confirming the reversible nature of the ortho metalation step. Eq. (2) outlines the stepwise relationship that exists between clusters **2b**, **2c**, and **3**.

(2)
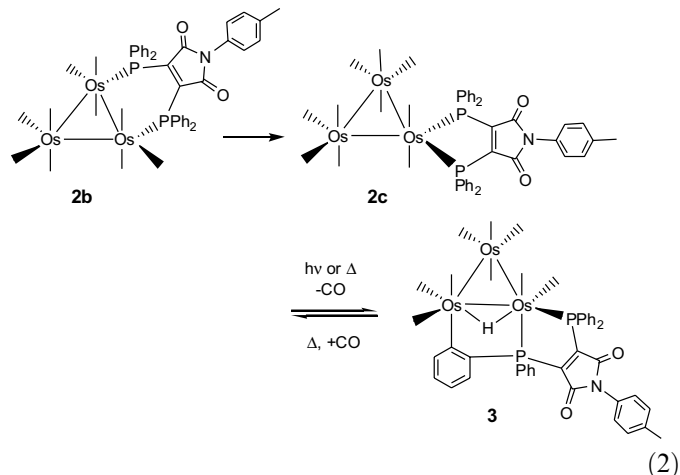
3.3. Isomerization kinetics for 1,2-Os$_3$(CO)$_{10}$(bmi) to 1,1-Os$_3$(CO)$_{10}$(bmi)

The isomerization of **2b** to **2c** was next investigated by UV–vis and ^{1}H NMR spectroscopies in toluene solution under 1 atm of CO, the latter whose presence is required to suppress the formation of the hydride cluster **3** [9,11e]. The isomerization was initially probed by ^{1}H NMR spectroscopy in toluene-d_8 at 323 K. Since all three methyl resonances appeared as non-overlapping singlets (**2b**: δ 1.83, **2c**: δ 1.98, **3**: δ 1.93), the extent of the reaction was easily followed from a plot of the total Os$_3$ concentration as a function of time. The NMR experiment confirmed that the transformation of **2b → 2c** proceeds completely to the chelating isomer and does not give rise to a equilibrium mixture containing **2b** and **2c** unlike the cluster compounds Os$_3$(CO)$_{10}$[(Z)-Ph$_2$PCH=CHPPh$_2$] and H$_4$Ru$_4$(CO)$_{10}$-(dppe) that we have studied and that exhibit dynamic equilibria in favor of the chelating isomer. The smooth exponential decay (**2b**) and growth (**2c**) curves afforded the first-order rate constant quoted in Table 3. Since the overall concentration for the hydride cluster **3** remained
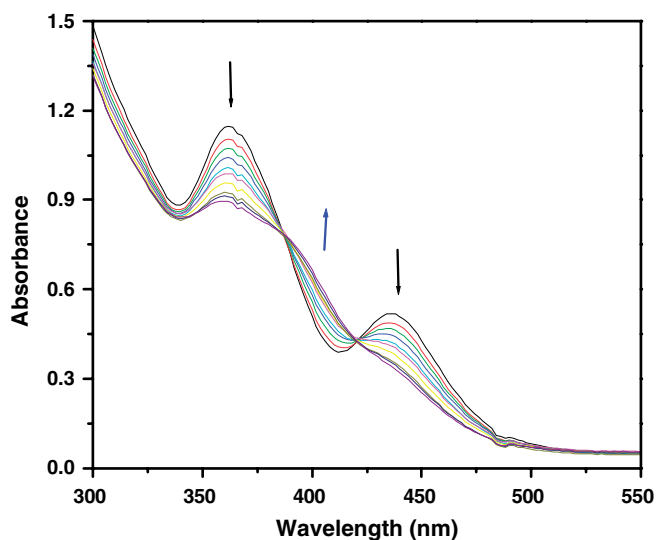

Fig. 2. UV–vis spectral changes for the photochemically promoted conversion of **2c → 3** in toluene at room temperature.

Table 3
Kinetic data for the isomerization of 1,2-Os$_3$(CO)$_{10}$(bmi) (**2b**) to 1,1-Os$_3$(CO)$_{10}$(bmi) (**2c**)[a]

Temperature (K)	Solvent	$10^5 k$ (s^{-1})[b]	Method
318.0	Toluene	1.86 ± 0.12	UV–vis
323.0	Toluene	3.24 ± 0.10	UV–vis
323.0	Toluene-d_8	3.53 ± 0.09	^{1}H NMR
333.0	Toluene	11.1 ± 0.2	UV–vis
333.0	Toluene	13.6 ± 0.3	UV–vis[c]
341.0	Toluene	25.00 ± 0.02	UV–vis
348.0	Toluene	52.80 ± 0.06	UV–vis

[a] All kinetic experiments were conducted under 1 atm of CO.
[b] The extent of the isomerization was followed by monitoring the increase in the absorbance of the 362 nm band (UV–vis) or the decrease in the initial intensity of the methyl singlet at δ 1.83 for 1,2-Os$_3$(CO)$_{10}$(bmi) (NMR).
[c] Reaction conducted in the presence of 10 equivalents of PPh$_3$.
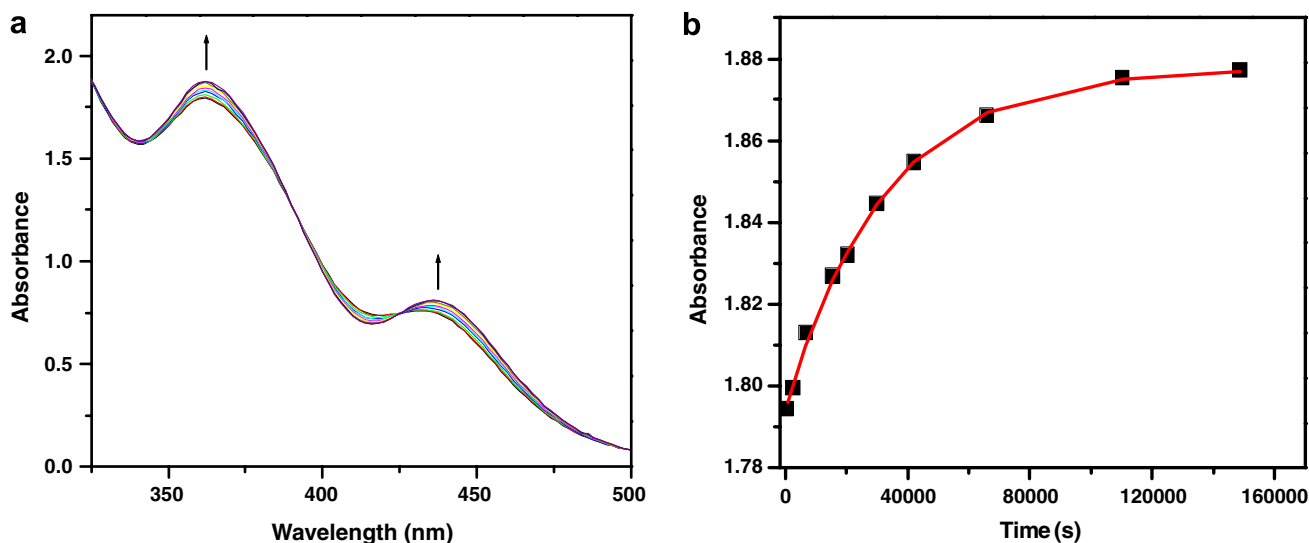
Fig. 3. UV–vis spectral changes for the isomerization of **2b** → **2c** in toluene at 323 K (a) and the absorbance versus time curve for the experimental data (■) and the least-squares fit of k (——, b).

essentially unchanged under these conditions, the data were also analyzed by a traditional ln[**2b**] versus time plot, which furnished a rate $[3.53(0.09) \times 10^{-5}\,\text{s}^{-1}]$ in excellent agreement to the rate obtained from the non-linear regression treatment of the data.

The UV–vis kinetic studies were conducted over the temperature range of 318–348 K, with the first-order rate constants reported in Table 3. Here the reaction rates were measured by following the increase in the absorbance of the 362 nm band belonging to **2c**. Fig. 3a shows the spectral changes that accompany the isomerization at 323 K, where the observed isosbestic points at 392 and 426 nm confirm that the isomerization is well-behaved and not subject to significant material loss. Inspection of Fig. 3b confirms the excellent fit between the least-squares regression curve and the absorbance data, yielding the quoted value in Table 3 that is within experimental error to the NMR determined rate. We also probed the effect of added phosphine on the isomerization reaction. Entries 4 and 5 in Table 3 confirm that the reaction rates under the standard conditions (1 atm CO) and added PPh3 (10 equiv.), respectively, are indistinguishable, ruling out a dissociative process leading to the generation of a long-lived unsaturated intermediate. An Eyring plot of $\ln(k/T)$ versus T^{-1} afforded activation parameters $[\Delta H^{\ddagger} = 24.0(0.1)\,\text{kcal/mol}$ and $\Delta S^{\ddagger} = -5(1)\,\text{eu}]$ that are in close agreement with those data published by us on the diphosphine ligand isomerization in $Os_3(CO)_{10}(P-P)$ [where $P-P = (Z)$-1,2-Ph2PCH=CHPPh2, bpcd] and $H_4Ru_4(CO)_{10}(dppe)$ [7b,9,11i]. The negative entropy of activation argues against a dissociative process involving the release of either a CO group or one arm of the bmi ligand. Our kinetic data are consistent with a unimolecular rearrangement where one of the phosphine moieties migrates across one of the Os–Os bonds by way of a μ-phosphine interme-

diate [31]. Coupled with this phosphine transit is the simultaneous migration of two equatorially situated CO ligands, as depicted in the merry-go-round process in Eq. (3) [32].

(3)
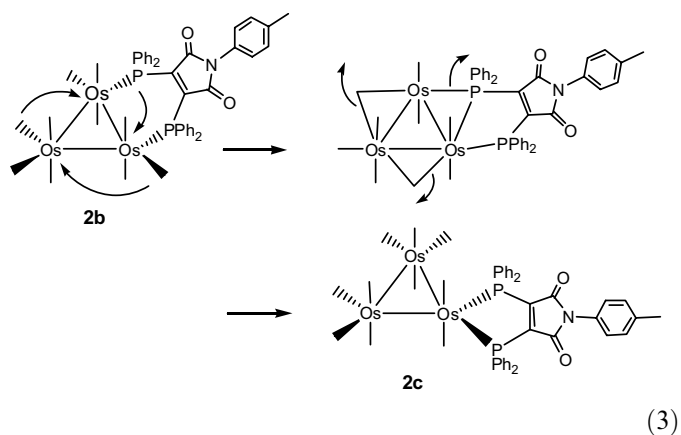
4. Conclusions

Displacement of the MeCN ligands in $1,2\text{-}Os_3(CO)_{10}$-$(MeCN)_2$ by the diphosphine ligand 2,3-bis(diphenylphosphino)-N-p-tolylmaleimide (bmi) produces the corresponding bmi-bridged cluster $1,2\text{-}Os_3(CO)_{10}(bmi)$ (**2b**) as the major product. Cluster **2b** undergoes a nondissociative isomerization of the ancillary bmi ligand to give the bmi-chelated cluster $1,1\text{-}Os_3(CO)_{10}(bmi)$ (**2c**). Photochemically promoted ortho metalation of **2c** is observed upon near-UV excitation to furnish the hydride-bridged cluster $HOs_3(CO)_9[\mu$-$(PPh_2)C=C\{PPh(C_6H_4)\}C(O)N(tolyl\text{-}p)C(O)]$ (**3**). All three clusters have been fully characterized bu IR and NMR (^{1}H and ^{31}P) spectroscopies, with the solid-state structure of **2c** established by X-ray crystallography.

Acknowledgment

Appendix A. Supporting information

Crystallographic data for the structural analysis have been deposited with the Cambridge Crystallographic Data Center: CCDC No. 606514 for **2c**. Copies of these data may be obtained free of charge from the Director, CCDC, 12 Union Road, Cambridge CB2 1EZ, UK [fax: +44 1223 336 033; e-mail: deposit@ccdc.ac.uk or www: http://www.ccdc.cam.ac.uk]. Supplementary data associated with this article can be found, in the online version, at doi:10.1016/j.jorganchem.2006.07.040.

References

[1] J.P. Collman, L.S. Hegedus, J.R. Norton, R.G. Finke, Principles and Applications of Organotransition Metal Chemistry, University Science Books, Mill Valley, CA, 1987.

[2] (a) A.L. Balch, B.J. Davies, M.M. Olmstead, J. Am. Chem. Soc. 112 (1990) 8592;
(b) A.L. Balch, B.J. Davies, M.M. Olmstead, Inorg. Chem. 32 (1993) 3937.

[3] (a) H. Werner, Angew. Chem., Int. Ed. 43 (2004) 938;
(b) T. Pechmann, C.D. Brandt, H. Werner, Chem. Commun. (2003) 1136;
(c) T. Pechmann, C.D. Brandt, H. Werner, Angew. Chem., Int. Ed. 39 (2000) 3909.

[4] M. Sauthier, B. Le Guennic, V. Deborde, L. Toupet, J.-F. Halet, R. Réau, Angew. Chem., Int. Ed. 40 (2001) 228.

[5] (a) S. Alvarez, G. Aullon, Met. Clust. Chem. 1 (1999) 308;
(b) E.R. Davidson, K.L. Kunze, F.B.C. Machado, S.J. Chakravorty, Acc. Chem. Res. 26 (1993) 628;
(c) C. De la Cruz, N. Sheppard, J. Mol. Struct. (1990) 141;
(d) C.P. Horwitz, D.F. Shriver, Adv. Organomet. Chem. 23 (1984) 219.

[6] For related studies dealing with the fluxional behavior of cluster-bound CO and isonitrile ligands, see: (a) B.E. Mann, Prog. NMR Spectrosc. 11 (1977) 95;
(b) S. Aime, L. Milone, Prog. NMR Spectrosc. 11 (1977) 183;
(c) J. Evans, Adv. Organomet. Chem. 16 (1977) 319;
(d) F.A. Cotton, B.E. Hanson, in: P. de Mayo (Ed.), Rearrangements in Ground and Excited States, Academic Press, New York, 1980 (Chapter 12).

[7] For H$_4$Ru$_4$(CO)$_{10}$(dppe), see: (a) M.R. Churchill, R.A. Lashewycz, J.R. Shapley, S.I. Richter, Inorg. Chem. 19 (1980) 1277;
(b) S. Kandala, M.G. Richmond, 45 (2006) in press.

[8] For PtRu$_5$(μ_6-C)(CO)$_{15}$(PMe$_2$Ph), see: R.D. Adams, B. Captain, W. Fu, P.J. Pellechia, Inorg. Chem. 42 (2003) 3111.

[9] For Os$_3$(CO)$_{10}$(bpcd), see: W.H. Watson, G. Wu, M.G. Richmond, Organometallics 25 (2006) 930.

[10] For related examples of phosphine ligand fluxionality, see: (a) K.A. Sutin, J.W. Kolis, M. Mlekuz, P. Bougeard, B.G. Sayer, M.A. Quilliam, R. Faggiani, C.J.L. Lock, M.J. McGlinchey, G. Jaouen, Organometallics 6 (1987) 439;
(b) A.M. Bradford, G. Douglas, L. Manojlović-Muir, K.W. Muir, R.J. Puddephatt, Organometallics 9 (1990) 409;
(c) P. Braunstein, J. Rosé, D. Toussaint, S. Jääskeläinen, M. Ahlgren, T.A. Pakkanen, J. Pursiainen, L. Toupet, D. Grandjean, Organometallics 13 (1994) 2472;

(d) G. Laurenczy, G. Bondietti, R. Ros, R. Roulet, Inorg. Chim. Acta 247 (1996) 65;
(e) S. Bouherour, P. Braunstein, J. Rosé, L. Toupet, Organometallics 18 (1999) 4908;
(f) R. Persson, M. Monari, R. Gobetto, A. Russo, S. Aime, M.J. Calhorda, E. Nordlander, Organometallics 20 (2001) 4150;
(g) Y. Ohki, H. Suzuki, Angew. Chem., Int. Ed. 41 (2002) 2994;
(h) R.D. Adams, B. Captain, W. Fu, J. Clust. Sci. 12 (2001) 303;
(i) W.H. Watson, G. Wu, M.G. Richmond, Organometallics 24 (2005) 5431;
(j) L.J. Pereira, W.K. Leong, J. Organomet. Chem. 691 (2006) 1941.

[11] (a) K. Yang, J.M. Smith, S.G. Bott, M.G. Richmond, Organometallics 12 (1993) 4779;
(b) H. Shen, S.G. Bott, M.G. Richmond, Organometallics 14 (1995) 4625;
(c) S.G. Bott, K. Yang, K.A. Talafuse, M.G. Richmond, Organometallics 22 (2003) 1383;
(d) S.G. Bott, H. Shen, R.A. Senter, M.G. Richmond, Organometallics 22 (2003) 1953;
(e) S.G. Bott, K. Yang, M.G. Richmond, J. Organomet. Chem. 690 (2005) 3067;
(f) W.H. Watson, S.G. Bodige, K. Ejsmont, J. Liu, M.G. Richmond, J. Organomet. Chem. 691 (2006) 3609.

[12] For the only known report between a N-phenylmaleimide-based diphosphine ligand and a metal cluster, see: K. Ejsmont, W.H. Watson, J. Liu, M.G. Richmond, J. Chem. Crystallogr. 33 (2003) 541.

[13] J.N. Nicholls, M.D. Vargas, Inorg. Synth. 26 (1989) 289.

[14] S.R. Drake, P.A. Loveday, Inorg. Synth. 28 (1990) 230.

[15] W.H. Watson, G. Wu, M.G. Richmond, J. Chem. Crystallogr. 33 (2003) 983.

[16] D.F. Shriver, The Manipulation of Air-Sensitive Compounds, McGraw-Hill, New York, 1969.

[17] (a) C.A. Parker, Proc. R. Soc. Lond. Ser. A 220 (1953) 104;
(b) C.G. Hatchard, C.A. Parker, Proc. R. Soc. Lond. Ser. A 235 (1956) 518.

[18] SAINT Version 6.02, Bruker Analytical X-ray Systems, Inc. Copyright 1997–1999.

[19] SHELXTL Version 5.1, Bruker Analytical X-ray Systems, Inc. Copyright 1998.

[20] A.L. Spek, PLATON – A Multipurpose Crystallographic Tool, Utrecht University, Utrecht, The Netherlands, 2001.

[21] All rate calculations were performed with the aid of the commercially available program ORIGIN-6.0. Here the initial (A_0) and final (A_∞) absorbances and the rate constant to equilibrium (k_e) were floated to give the quoted least-squares value for first-order rate constant k_e.

[22] B.K. Carpenter, Determination of Organic Reaction Mechanisms, Wiley–Interscience, New York, 1984.

[23] (a) P.E. Garrou, Chem. Rev. 81 (1981) 229;
(b) M.G. Richmond, J.K. Kochi, Organometallics 6 (1987) 254.

[24] W.H. Watson, B. Poola, M.G. Richmond, J. Chem. Crystallogr. 36 (2006) 123.

[25] We have intentionally avoided heating clusters **2b**, **2c**, and **3** at temperatures higher than 353 K in order to prevent the formation of benzyne-substituted clusters through P–Ph bond activation (see Ref. [9]).

[26] N.B. Colthup, L.H. Daly, S.E. Wiberley, Introduction to Infrared and Raman Spectroscopy, third ed., Academic Press, New York, 1990.

[27] (a) M.R. Churchill, B.G. DeBoer, Inorg. Chem. 16 (1977) 878;
(b) M.I. Bruce, G.N. Pain, C.A. Hughes, J.M. Patrick, B.W. Skelton, A.H. White, J. Organomet. Chem. 307 (1986) 343;
(c) R.D. Adams, J.T. Tanner, Organometallics 8 (1989) 563;
(d) K. Biradha, V.M. Hansen, W.K. Leong, R.K. Pomeroy, M. Zaworotko, J. Clust. Sci. 11 (2000) 285;
(e) A.J. Deeming, M. Stchedroff, J. Chem. Soc., Dalton Trans. (1998) 3819;

(f) A.J. Deeming, M.M. Hassan, S.E. Kabir, E. Nordlander, D.A. Tocher, J. Chem. Soc., Dalton Trans. (2004) 3709.

[28] M.I. Bruce, M.J. Liddell, C.A. Hughes, B.W. Skelton, A.H. White, J. Organomet. Chem. 347 (1988) 157.

[29] (a) K. Yang, S.G. Bott, M.G. Richmond, Organometallics 13 (1994) 3788;
(b) H. Shen, T.J. Williams, S.G. Bott, M.G. Richmond, J. Organomet. Chem. 505 (1995) 1;
(c) S.G. Bott, K. Yang, J.C. Wang, M.G. Richmond, Inorg. Chem. 39 (2000) 6051;
(d) S.G. Bott, H. Shen, M.G. Richmond, J. Organomet. Chem. 689 (2004) 3426.

[30] The ortho metalation reaction leading to cluster **3**, and with it the chelation of the ancillary bmi ligand at axial and equatorial sites at the osmium center, is strengthened by the X-ray diffraction structure of the related hydride-bridged cluster $HOs_3(CO)_9[\mu\text{-}(PPh_2)C=C\{PPh(C_6H_4)\}C(O)C(=CHFc)C(O)]$. Unpublished results.

[31] Analogous μ-phosphine-bridged intermediates have been invoked in the other known examples that proceed by a *bona fide* nondissociative rearrangement. See Refs. [9,10].

[32] Our kinetic data do not rule out the participation of the doubly bridged cluster species $Os_3(CO)_9(\mu\text{-}CO)(\mu\text{-}bmi)$ in the isomerization reaction. However, we do not favor this route because the pairwise exchange of the CO/P groups across the osmium-osmium bond requires an additional turnstile rotation or permutation of the two CO groups and the two phosphorus groups at the bmi-chelated osmium center in order to furnish $1,1\text{-}Os_3(CO)_{10}(bmi)$ with equatorially disposed phosphine groups (vide supra the X-ray structure of **2c**).